INTERNATIONAL JOURNAL OF PHARMACEUTICAL SCIENCES
[ISSN: 0975-4725; CODEN(USA): IJPS00]
Journal Homepage: https://www.ijpsjournal.com

OPEN ACCESS

Research Paper

Extracellular Mycogenic Synthesis of Silver Nanoparticles Using Indigenous White-Rot Fungi Ganoderma lucidum and Pleurotus ostreatus Characterization and Antimicrobial Potential

Dr. Boddireddy Sridevi*, Mamatha Mallavajhala

Telangana Social Welfare Residential College for Women, Warangal East, Warangal–506005, Telangana, India.

ARTICLE INFO

Published: 12 Sept 2026
Keywords:
Silver nanoparticles; mycogenic synthesis; white-rot fungi; Ganoderma lucidum; Pleurotus ostreatus; extracellular biosynthesis; UV–Visible spectroscopy; FTIR; antibacterial activity; green nanotechnology
DOI:
10.5281/zenodo.22723271

ABSTRACT

The search for environmentally compatible routes for the production of metallic nanoparticles has increased interest in fungal-mediated synthesis. Fungi are particularly useful biological platforms because their extracellular secretome contains enzymes, proteins, peptides, polysaccharides and low-molecular-weight metabolites that may participate in metal-ion reduction and nanoparticle stabilization. The present study investigated extracellular synthesis of silver nanoparticles (AgNPs) using indigenous white-rot fungal isolates identified morphologically as Ganoderma lucidum and Pleurotus ostreatus. Fruiting bodies collected from hardwood-associated material in Warangal, Telangana, India, were established on malt extract agar and propagated in malt extract broth. Cell-free mycelial extracts were prepared after aqueous extraction of washed biomass and reacted with 1 mM $AgNO_3$ for 48 h at 180 rpm. Nanoparticle formation was indicated by development of a reddish-brown colour, whereas the $AgNO_3$ control remained unchanged. UV–Visible spectra showed broad maxima at approximately 450 nm for both fungal preparations. Figure-derived peak absorbances were approximately 1.66 for the Ganoderma preparation and 0.92 for the Pleurotus preparation. FTIR spectra displayed bands in the approximate 2920, 1640, 1380 and 1050–1100 cm^{-1} regions, supporting the association of fungal-derived organic functionalities with the nanoparticle preparations. In agar well diffusion assays, both AgNP preparations inhibited Escherichia coli, Klebsiella pneumoniae, Staphylococcus aureus and Bacillus subtilis. The largest recorded inhibition zone was 10 mm for Pleurotus-derived AgNPs against K. pneumoniae, while Ganoderma-derived AgNPs produced 8 mm against S. aureus.

***Corresponding Author:** Dr. Boddireddy Sridevi
Address: *Department of Microbiology*, *Telangana Social Welfare Residential College for Women, Warangal East, Warangal–506005, Telangana, India.*
Email ✉: mula.bsridevi@gmail.com

Relevant conflicts of interest/financial disclosures: The authors declare that the research was conducted in the absence of any commercial or financial relationships that could be construed as a potential conflict of interest.

INTRODUCTION

Nanotechnology enables the design and investigation of materials whose physicochemical behaviour differs from that of their bulk counterparts. Among metallic nanomaterials, silver nanoparticles (AgNPs) have attracted sustained attention because of their optical properties, high surface-area-to-volume ratio and broad antimicrobial activity. These properties have encouraged investigation of AgNPs in antimicrobial surfaces, coatings, packaging, environmental technologies, biosensing and biomedical applications [1,2].

Conventional physical and chemical routes can provide control over nanoparticle formation, but may involve substantial energy requirements, elevated temperatures or pressures, and synthetic reducing or stabilizing agents. Biological synthesis has consequently been investigated as an alternative in which microorganisms, plants or biological extracts provide reducing and capping components under comparatively mild aqueous conditions [1,3]. Extracellular synthesis is especially attractive because nanoparticles formed in the reaction medium are potentially easier to recover than particles accumulated intracellularly [4–6].

Fungi are promising biological nanofactories because they can generate substantial biomass and secrete diverse extracellular biomolecules. Proteins, enzymes, peptides, polysaccharides, amino acids and secondary metabolites may contribute to reduction of Ag^{+} to Ag^{0} and subsequently remain associated with the nanoparticle surface as a biological capping layer. Recent reviews emphasize that variability in fungal secretomes is an important determinant of synthesis kinetics, surface chemistry, stability and reproducibility [2,3].

White-rot fungi are particularly interesting because their ecological and physiological adaptation to lignocellulosic substrates involves extensive extracellular oxidative enzyme systems. Laccases, peroxidases, reductases and other secreted metabolites may provide chemically active environments capable of interacting with metal ions. Earlier work has demonstrated extracellular AgNP synthesis using several fungi, including *Fusarium oxysporum*, *Aspergillus fumigatus* and white-rot fungal culture filtrates [4–7]. Gudikandula *et al*. reported extracellular AgNP synthesis using white-rot fungi, with plasmon peaks around 419–421 nm and TEM-confirmed particles in the 15–25 nm range, illustrating the relevance of white-rot fungi to mycogenic nanomaterial production [4].

The antimicrobial behaviour of AgNPs is generally attributed to several interacting processes rather than to a single mechanism. These include adsorption to bacterial cell envelopes, disruption of membrane integrity, release of Ag^{+} ions, oxidative stress and reactive oxygen species generation, inhibition of respiratory enzymes and interaction with proteins and nucleic acids [8–10]. The magnitude of activity can vary with particle size, morphology, surface chemistry, aggregation state, Ag^{+} release and the test organism [1,8,9].

The present work examines two indigenous white-rot fungal isolates, *Ganoderma lucidum* and *Pleurotus ostreatus*, collected in Warangal, Telangana, as extracellular platforms for AgNP synthesis. The experimental workflow integrates fungal isolation and cultivation, preparation of cell-free mycelial extract, reaction with $AgNO_3$, visual monitoring, UV–Visible spectroscopy, FTIR analysis and preliminary antibacterial evaluation.

1.1 Objectives

• To isolate and establish indigenous white-rot fungal cultures provisionally identified as Ganoderma lucidum and Pleurotus ostreatus.

• To prepare cell-free mycelial extracts and assess their ability to reduce Ag^+ ions extracellularly.
• To monitor AgNP formation by visual colour change and UV–Visible spectroscopy.
• To examine the functional groups associated with the synthesized nanoparticle preparations using FTIR spectroscopy.
• To evaluate preliminary antibacterial activity against selected Gram-negative and Gram-positive bacteria using agar well diffusion.

2. MATERIALS AND METHODS

2.1 Collection and preliminary identification of fungi

Indigenous white-rot fungal fruiting bodies were collected from hardwood-associated material in Warangal, Telangana, India. Two isolates were designated *Ganoderma* sp. and *Pleurotus* sp. and are referred to in this manuscript as *Ganoderma lucidum* and *Pleurotus ostreatus* based on preliminary macromorphological identification. Characters considered included growth habit, attachment, pileus morphology, colour, lamellae or pore-bearing surface, stipe characteristics and spore-associated features.

Figure 1. Representative fruiting-body material used for fungal isolation and culture establishment: (A) Ganoderma lucidum fruiting body; (B) Pleurotus ostreatus fruiting body.

2.2 Establishment and maintenance of pure cultures

Approximately 10 mg of internal fungal tissue was aseptically excised from fruiting bodies and transferred to malt extract agar (MEA) containing malt extract (30.0 g L^{-1}) and mycological peptone (5.0 g L^{-1}), with the pH adjusted to approximately 5.5. Plates were sealed with Parafilm and incubated at room temperature. Emerging colonies were subcultured to obtain pure cultures and maintained on MEA slants at 4 °C.

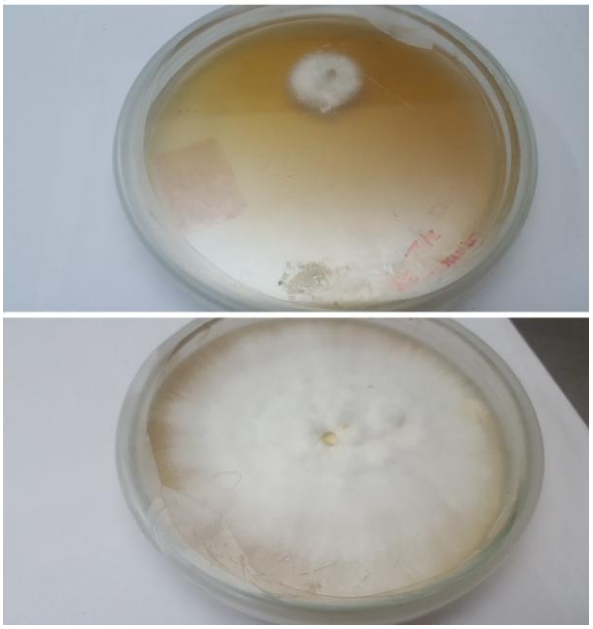

Figure 2. Representative *Ganoderma lucidum* growth during culture establishment

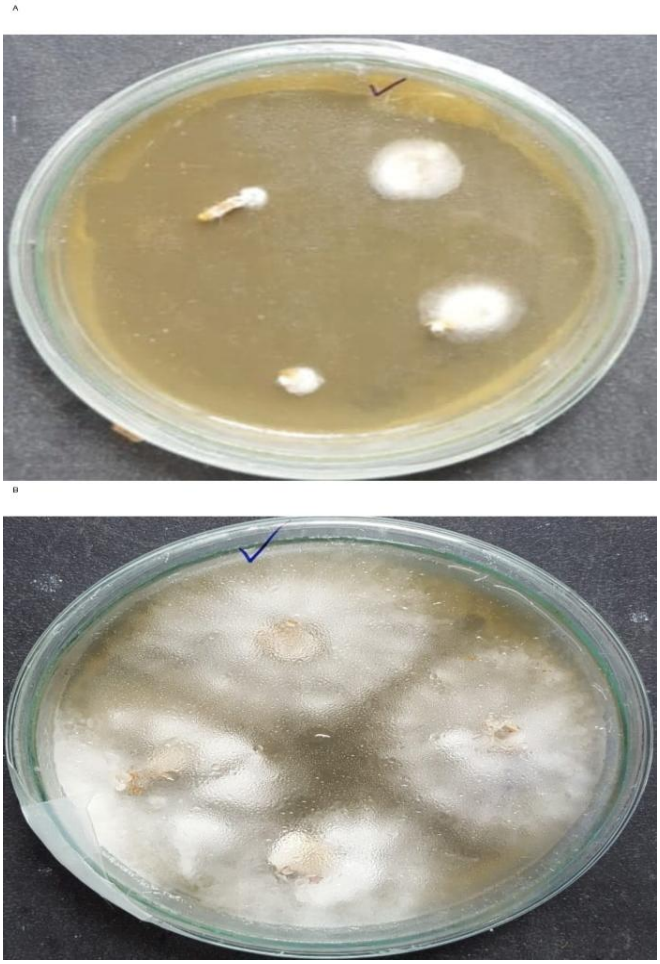

Figure 3. Representative culture plates showing development of fungal mycelia used for subsequent biomass production: *Pleurotus ostreatus* culture.

2.3 Biomass production and preparation of cell-free mycelial extract

Established fungal cultures were propagated in malt extract broth and incubated on an orbital shaker at 180 rpm for three days. Biomass was recovered by filtration and washed repeatedly with deionized water to reduce residual medium components. The washed biomass was suspended in 100 mL deionized water and maintained under shaking conditions for 72 h to facilitate release of extracellular biomolecules. The suspension was then filtered through Whatman No. 1 filter paper to obtain the cell-free mycelial extract used for AgNP synthesis. This extracellular approach is consistent with established fungal biosynthesis strategies in which secreted proteins and other metabolites participate in Ag^{+} reduction and nanoparticle stabilization [4–7].

Figure 4. Representative culture tubes used for maintenance of the fungal isolates: (A)*G. lucidum* and (B) *P. ostreatus* fungal cultures maintained on laboratory medium.

2.4 Extracellular synthesis of AgNPs

The cell-free mycelial extract was mixed with aqueous $AgNO_3$ to obtain a final concentration of 1 mM. Reaction mixtures were incubated at 180 rpm for 48 h. An $AgNO_3$-only control lacking fungal extract was maintained under comparable conditions. Formation of AgNPs was monitored initially through visible colour development. The change from pale yellow to reddish-brown was interpreted as preliminary evidence of colloidal silver formation, consistent with the optical behaviour reported for biologically synthesized AgNPs [4–7].

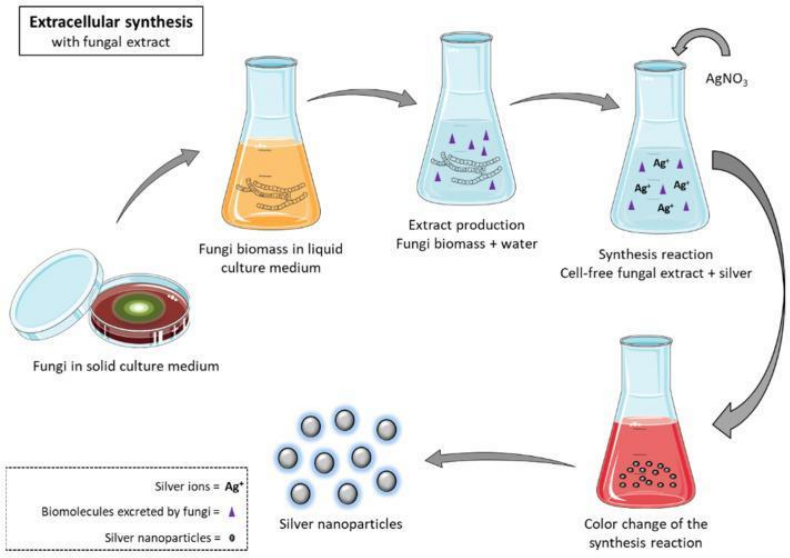

Figure 5. Schematic workflow for extracellular mycogenic synthesis of AgNPs using fungal biomass, aqueous extraction, $AgNO_3$ reduction and formation of colloidal silver nanoparticles.

2.5 UV–Visible spectroscopy

UV–Visible spectroscopy was used to evaluate the optical response of the synthesized preparations. The reported λmax and absorbance values were read from the supplied plotted spectrum because the original instrument-exported data file was not available. Accordingly, the values are reported as approximate figure-derived measurements and should be replaced by the instrument-generated numerical values before submission to a journal. Surface plasmon resonance (SPR) in the visible region is a commonly used preliminary indicator of AgNP formation and is influenced by particle size, morphology, aggregation and the local refractive environment [1,4].

2.6 FTIR spectroscopy

FTIR spectroscopy was used to identify functional groups associated with biomolecules retained on or interacting with the AgNP preparations. The supplied spectra were obtained using a Bruker instrument. Peak positions were interpreted approximately from the plotted spectra; exact numerical peak maxima should be obtained from the original instrument report. FTIR assignments were therefore treated as tentative rather than definitive, particularly in regions where multiple biomolecular functional groups can overlap [4,7].

2.7 Antibacterial activity

Antibacterial activity was evaluated by agar well diffusion against *Escherichia coli*, *Klebsiella pneumoniae, Staphylococcus aureus* and *Bacillus subtilis*. The study record contains inhibition-zone values for *Ganoderma*-derived AgNPs, *Pleurotus*-derived AgNPs, fungal culture filtrate and a standard antibiotic. Agar diffusion is an established screening method, but the magnitude of an inhibition zone is influenced by diffusion, inoculum, medium composition, incubation conditions and agent concentration [11].

2.8 Statistical treatment and data-quality considerations

Descriptive comparisons were calculated from the supplied single observations. The difference between the two UV–Visible peak absorbances was calculated as 1.66 − 0.92 = 0.74 absorbance units, and the relative difference was

approximately 80.4% when the *Pleurotus* value was used as the reference.

3. Results

3.1 Isolation and culture establishment

The collected fruiting-body material yielded two fungal isolates that were successfully established on malt extract medium. The supplied photographs show active mycelial growth and subsequent maintenance cultures. Successful establishment of stable cultures provided the biomass required for preparation of cell-free extracts and subsequent extracellular AgNP synthesis (Figures 1–4).

3.2 Visual evidence of AgNP formation

Following addition of fungal cell-free extracts to 1 mM $AgNO_3$, the reaction mixtures developed a reddish-brown colour within approximately 48 h, whereas the $AgNO_3$ control did not show the same colour transition (Figure 9). Such colour development is a widely reported preliminary observation during AgNP formation and is associated with the collective optical response of nanoscale silver particles [4–7]. Although colour change alone does not establish particle size or morphology, its occurrence together with the observed SPR band provides convergent preliminary evidence for nanoparticle formation.

Figure 9. Representative reaction flasks showing the fungal extracts and the visible colour development observed during extracellular AgNP synthesis.

3.3 UV–Visible spectral characteristics

Fungal preparation	$AgNO_3$	Reaction time	Observed λmax (nm)	Approx. peak absorbance
Ganoderma-derived AgNPs	1 mM	48 h	~450	~1.66
Pleurotus-derived AgNPs	1 mM	48 h	~450	~0.92

Both preparations exhibited a broad optical maximum centred at approximately 450 nm (Figure 6). The *Ganoderma*-derived preparation showed a substantially higher peak absorbance than the *Pleurotus*-derived preparation. The absolute difference was 0.74 absorbance units, corresponding to approximately 80.4% higher absorbance relative to the *Pleurotus* preparation. This observation should not be interpreted as an 80.4% higher nanoparticle yield because absorbance is affected by particle concentration, size distribution, morphology, aggregation, path length and the refractive environment [1,4].

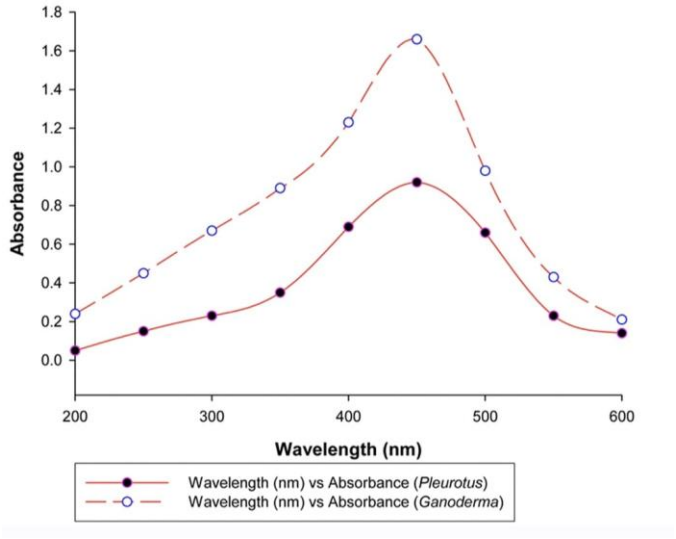

Figure 6. UV–Visible absorption spectra of AgNP preparations synthesized using *Ganoderma lucidum* and *Pleurotus ostreatus* mycelial extracts. Both preparations show a broad maximum near 450 nm, with higher absorbance for the *Ganoderma*-derived preparation.

3.4 FTIR characteristics

Approx. band (cm^{-1})	Tentative assignment	Interpretation
~2920	Aliphatic C–H stretching	Organic fungal constituents associated with the particle surface
~1640	Amide I/C=O and/or H–O–H bending region	Protein-associated or adsorbed biomolecular contribution
~1380	C–N/O–H-associated deformation region	Possible protein, amino-acid or carbohydrate contribution
~1050–1100	C–O/C–O–C stretching	Polysaccharides and other oxygenated metabolites
~500–600	Fingerprint/inorganic-associated region	Changes associated with the nanoparticle surface environment

Both spectra contained features in the C–H, amide/carbonyl, deformation and carbohydrate-associated regions (Figures 7 and 8). A prominent feature near approximately 1380 cm^{-1} occurred in both preparations. The similarity suggests that fungal-derived organic molecules remained associated with the nanoparticle preparations. However, because exact peak maxima and appropriate fungal-extract controls were not supplied, these assignments remain tentative and should not be presented as proof of a specific enzyme or metabolite.

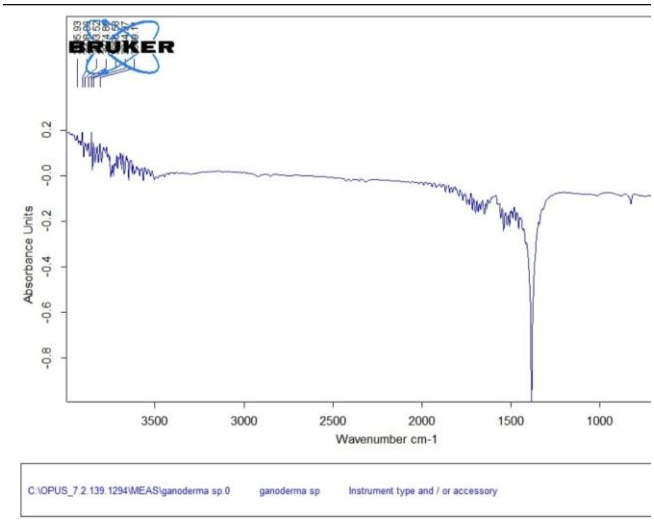

Figure 7. FTIR spectrum of the *Ganoderma*-derived AgNP preparation, showing prominent mid-infrared absorption features associated with fungal-derived organic functionalities.

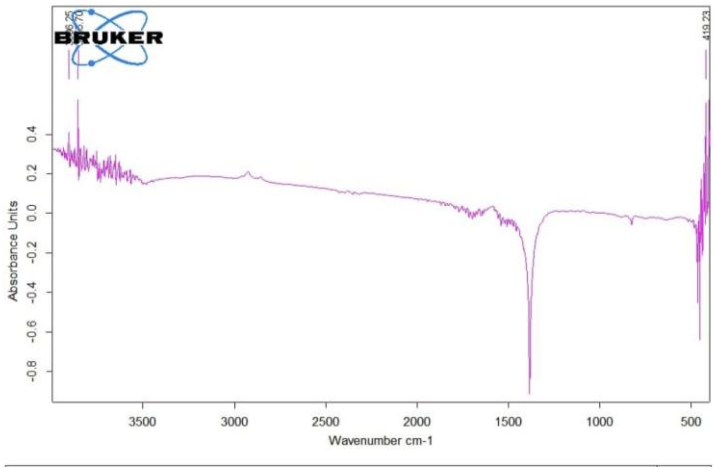

Figure 8. FTIR spectrum of the *Pleurotus*-derived AgNP preparation, showing characteristic absorption features in regions associated with fungal proteins, carbohydrates and other organic constituents.

3.5 Antibacterial activity

Test organism	Ganoderma AgNPs (mm)	Pleurotus AgNPs (mm)	Culture filtrate (mm)	Standard antibiotic (mm)
E. coli	6	8	0.5	16
K. pneumoniae	5	10	1.2	20
S. aureus	8	6	0.8	14
B. subtilis	5	6	0.3	12

Both fungal AgNP preparations inhibited all four test organisms in the supplied agar-well dataset. *Pleurotus*-derived AgNPs produced the largest inhibition zone observed among the AgNP treatments against *K. pneumoniae* (10 mm), followed by 8 mm against *E. coli*. *Ganoderma*-derived AgNPs produced 8 mm against S. aureus and 6 mm against *E. coli*. Against *B. subtilis*, *Pleurotus* and *Ganoderma* preparations produced 6 and 5 mm, respectively. The culture filtrate alone

produced much smaller zones (0.3–1.2 mm), whereas the standard antibiotic produced substantially larger zones (12–20 mm).

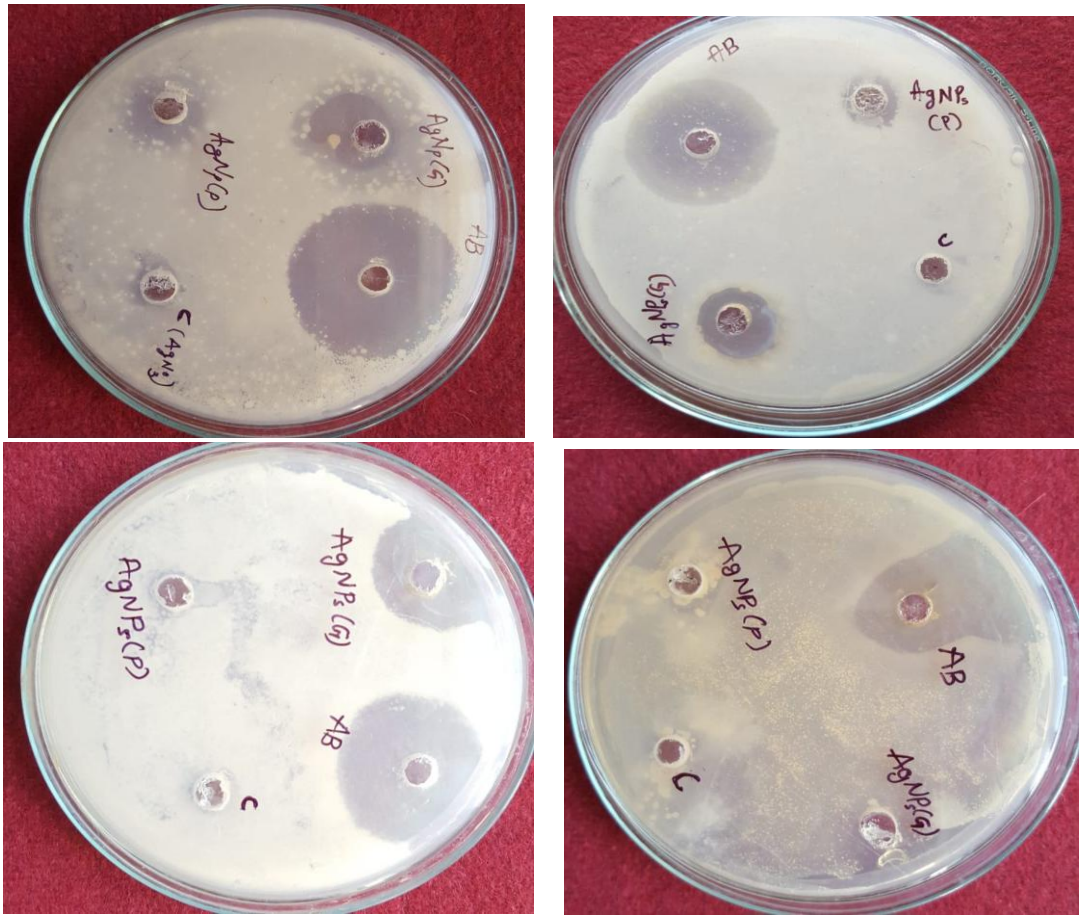

Figure 9: Antimicrobial activity of *Ganoderma* and *Pleurotus*-derived AgNPs

DISCUSSION

The present investigation provides preliminary experimental evidence that cell-free extracts from two indigenous white-rot fungal isolates can mediate extracellular formation of AgNPs under the tested aqueous conditions. The reddish-brown colour development, combined with broad UV–Visible absorption near 450 nm, is consistent with the formation of plasmonically active silver nanostructures. Fungal extracellular synthesis is well established as a green approach because secreted enzymes and metabolites can contribute to metal-ion reduction and stabilization [2–7].

The use of white-rot fungi is particularly relevant. Their secretomes contain oxidative and reductive enzymes and diverse metabolites associated with lignocellulose transformation. Recent systematic analysis indicates that fungal AgNP formation can involve both extracellular and intracellular pathways and that nitrate reductases, dehydrogenases, laccases and other oxidoreductases, together with proteins and polysaccharides, may contribute to reduction and capping [3]. The present FTIR observations are compatible with this multi-component interpretation, although the available data cannot identify which individual biomolecules were responsible.

The UV–Visible response provides a useful comparison between the two fungal systems. Both preparations exhibited an approximate maximum near 450 nm, but the *Ganoderma* preparation had a markedly greater absorbance (1.66 versus 0.92). Earlier work with white-rot fungi reported SPR maxima around 419–421 nm and TEM-confirmed particle sizes of approximately 15–25 nm [4]. The longer-wavelength and relatively broad response in the present spectra may reflect differences in particle size distribution, aggregation, surface capping or local dielectric environment.

The difference in absorbance also should not be equated with nanoparticle yield. According to Beer–Lambert behaviour, absorbance depends on concentration and optical path length, while the extinction coefficient of nanoparticles varies with size, shape and dielectric environment. Biological capping and aggregation can further modify the spectral response [1,4]. Thus, the higher *Ganoderma* absorbance suggests a stronger optical extinction response under the tested conditions, but quantitative nanoparticle yield requires mass balance, silver-content determination or a validated calibration approach.

FTIR analysis supports the presence of fungal organic components associated with the AgNP preparations. The approximate bands around 2920, 1640, 1380 and 1050–1100 cm^{-1} can be associated with aliphatic C–H, amide/carbonyl, deformation and C–O/C–O–C-containing functionalities, respectively. Such biomolecules may act as reducing agents, ligands or stabilizers. Nevertheless, the ~1380 cm^{-1} region can contain overlapping contributions, and FTIR alone cannot identify a specific enzyme, protein or metabolite. Comparison with spectra of the fungal extract before nanoparticle formation would strengthen the interpretation [4,7].

The antibacterial results are consistent with the broad antimicrobial behaviour described for AgNPs. Proposed mechanisms include interaction with bacterial cell envelopes, membrane perturbation, Ag^{+} release, oxidative stress and reactive oxygen species formation, inhibition of respiratory enzymes and interaction with proteins and DNA [8–10]. The species-dependent pattern observed here may reflect differences in cell-envelope structure and susceptibility, as well as nanoparticle diffusion and surface chemistry. *Pleurotus*-derived AgNPs were more active than *Ganoderma*-derived AgNPs against *E. coli* and *K. pneumoniae*, whereas *Ganoderma*-derived AgNPs showed greater inhibition against *S. aureus*. These differences emphasize that antimicrobial performance is not determined solely by the presence of silver but also by the physicochemical properties of the nanoparticle preparation. The culture filtrate controls produced very small inhibition zones, which is compatible with the interpretation that the observed antibacterial effect was associated mainly with the AgNP-containing preparations.

CONCLUSIONS

The study demonstrates the feasibility of extracellular mycogenic synthesis of AgNP preparations using indigenous white-rot fungal isolates identified provisionally as *Ganoderma lucidum* and *Pleurotus ostreatus*. Reaction of cell-free fungal extracts with 1 mM $AgNO_3$ for 48 h produced a reddish-brown colour and broad UV–Visible maxima near 450 nm. The figure-derived maximum absorbance was approximately 1.66 for the Ganoderma preparation and 0.92 for the *Pleurotus* preparation. FTIR spectra indicated the association of protein-, carbohydrate- and other oxygen/nitrogen-containing organic functionalities with the nanoparticle preparations. Both preparations showed preliminary antibacterial activity against *E. coli, K. pneumoniae, S. aureus* and *B. subtilis*.

REFERENCES

1. Gong X, Jadhav ND, Lonikar VV, Kulkarni AN, Zhang H, Sankapal BR, et al. An overview of green synthesized silver nanoparticles towards bioactive antibacterial, antimicrobial and antifungal applications. Advances in Colloid and Interface Science. 2024;323:103053. doi:10.1016/j.cis.2023.103053.
2. Alavi M, Ashengroph M. Mycosynthesis of AgNPs: mechanisms of nanoparticle formation and antimicrobial activities. Expert Review of Anti-infective Therapy. 2023;21(4):355–363. doi:10.1080/14787210.2023.2179988.
3. Chaurasia PK, Bharati S, Yadava S. Fungi and their extracellular/intracellular macromolecules in AgNPs production: A holistic systematic review. Process Biochemistry. 2026;166:167–190. doi:10.1016/j.procbio.2026.04.009.
4. Gudikandula K, Vadapally P, Singara Charya MA. Biogenic synthesis of silver nanoparticles from white rot fungi: Their characterization and antibacterial studies. OpenNano. 2017;2:64–78. doi:10.1016/j.onano.2017.07.002.
5. Ahmad A, Mukherjee P, Senapati S, Mandal D, Khan MI, Kumar R, Sastry M. Extracellular biosynthesis of silver nanoparticles using the fungus Fusarium oxysporum. Colloids and Surfaces B: Biointerfaces. 2003;28(4):313–318. doi:10.1016/S0927-7765(02)00174-1.
6. Duran N, Marcato PD, Alves OL, De Souza GIH, Esposito E. Mechanistic aspects of biosynthesis of silver nanoparticles by several Fusarium oxysporum strains. Journal of Nanobiotechnology. 2005;3:8. doi:10.1186/1477-3155-3-8.
7. Bhainsa KC, D'Souza SF. Extracellular biosynthesis of silver nanoparticles using the fungus Aspergillus fumigatus. Colloids and Surfaces B: Biointerfaces. 2006;47(2):160–164. doi:10.1016/j.colsurfb.2005.11.026.
8. Rai M, Yadav A, Gade A. Silver nanoparticles as a new generation of antimicrobials. Biotechnology Advances. 2009;27(1):76–83. doi:10.1016/j.biotechadv.2008.09.002.
9. Silver S. Bacterial silver resistance: molecular biology and uses and misuses of silver compounds. FEMS Microbiology Reviews. 2003;27(2–3):341–353. doi:10.1016/S0168-6445(03)00055-0.
10. More PR, Pandit S, De Filippis A, Franci G, Mijakovic I, Galdiero M. Silver nanoparticles: bactericidal and mechanistic approach against drug resistant pathogens. Microorganisms. 2023;11(2):369. doi:10.3390/microorganisms11020369.
11. Balouiri M, Sadiki M, Ibnsouda SK. Methods for in vitro evaluating antimicrobial activity: A review. Journal of Pharmaceutical Analysis. 2016;6(2):71–79. doi:10.1016/j.jpha.2015.11.005.
12. Bamal D, Singh A, Chaudhary G, Kumar M, Singh M, Rani N, Mundlia P, Sehrawat AR. Silver nanoparticles biosynthesis, characterization, antimicrobial activities, applications, cytotoxicity and safety issues: an updated review. Nanomaterials. 2021;11(8):2086. doi:10.3390/nano11082086.
13. Sun Y, Xia Y. Shape-controlled synthesis of gold and silver nanoparticles. Science. 2002;298(5601):2176–2179. doi:10.1126/science.1077229.
14. Basavaraja S, Balaji SD, Lagashetty A, Rajasab AH, Venkataraman A. Extracellular biosynthesis of silver nanoparticles using the fungus Fusarium semitectum. Materials Research Bulletin. 2008;43(5):1164–1170.

15. Birla SS, Gaikwad SC, Gade AK, Rai MK. Rapid synthesis of silver nanoparticles from Fusarium oxysporum by optimizing physicocultural conditions. The Scientific World Journal. 2013;2013:796018. doi:10.1155/2013/796018.
16. Balagna C, Perero S, Percivalle E, et al. Silver nanoparticles: Review of antiviral properties, mechanism of action and applications. Microorganisms. 2023;11(3):629. doi:10.3390/microorganisms11030629.

HOW TO CITE: Dr. Boddireddy Sridevi, Mamatha Mallavajhala, Extracellular Mycogenic Synthesis of Silver Nanoparticles Using Indigenous White-Rot Fungi Ganoderma lucidum and Pleurotus ostreatus Characterization and Antimicrobial Potential, Int. J. of Pharm. Sci., 2026, Vol 4, Issue 9, 1494-1506, https://doi.org/10.5281/zenodo.22723271